Biomedicine & Pharmacotherapy 135 (2021) 111186

Contents lists available at ScienceDirect

Biomedicine & Pharmacotherapy

journal homepage: www.elsevier.com/locate/biopha

# Novel *N,N*-di-alkylnaphthoimidazolium derivative of β-lapachone impaired *Trypanosoma cruzi* mitochondrial electron transport system

Ana Cristina S. Bombaça [a,1], Leonardo A. Silva [b,1], Otávio Augusto Chaves [b], Lorrainy S. da Silva [b], Juliana M.C. Barbosa [a], Ari M. da Silva [c], Aurélio B.B. Ferreira [b,2], Rubem F.S. Menna-Barreto [a,*]

[a] Laboratório de Biologia Celular, Instituto Oswaldo Cruz, Fundação Oswaldo Cruz, Rio de Janeiro, Brazil
[b] Instituto de Química, Universidade Federal Rural do Rio de Janeiro, Rio de Janeiro, Brazil
[c] Instituto de Pesquisa em Produtos Naturais, Universidade Federal do Rio de Janeiro, Rio de Janeiro, Brazil

ARTICLE INFO

This work is dedicated to the memory of the honorable Brazilian scientist, teacher, friend and human being Dr. Aurelio Ferreira (1945–2020)

*Keywords:*
*Trypanosoma cruzi*
Chemotherapy
Naphthoimidazoles
Mitochondria
Oxidative stress
Succinate dehydrogenase

ABSTRACT

*Trypanosoma cruzi* is a protozoan parasite that causes Chagas disease, a neglected tropical disease that is endemic in Latin America and spreading worldwide due to globalization. The current treatments are based on benznidazole and nifurtimox; however, these drugs have important limitations and limited efficacy during the chronic phase, reinforcing the necessity of an alternative chemotherapy. For the last 30 years, our group has been evaluating the biological activity of naphthoquinones and derivatives on *T. cruzi*, and of the compounds tested, N1, N2 and N3 were found to be the most active *in vitro*. Here, we show the synthesis of a novel β-lapachone-derived naphthoimidazolium named N4 and assess its activity on *T. cruzi* stages and the mechanism of action. The new compound was very active on all parasite stages ($IC_{50}$/24 h in the range of 0.8–7.9 μM) and had a selectivity index of 5.4. Mechanistic analyses reveal that mitochondrial ROS production begins after short treatment starts and primarily affects the activity of complexes II-III. After 24 h treatment, a partial restoration of mitochondrial physiology (normal complexes II-III and IV activities and controlled $H_2O_2$ release) was observed; however, an extensive injury in its morphology was still detected. During treatment with N4, we also observed that trypanothione reductase activity increased in a time-dependent manner and concomitant with increased oxidative stress. Molecular docking calculations indicated the ubiquinone binding site of succinate dehydrogenase as an important interaction point with N4, as with the FMN binding site of dihydroorotate dehydrogenase. The results presented here may be a good starting point for the development of alternative treatments for Chagas disease and for understanding the mechanism of naphthoimidazoles in *T. cruzi*.

## 1. Introduction

Even 110 years after its discovery, Chagas disease is still a serious public health problem, related to poverty and endemic in Latin American countries. It is a neglected disease, caused by the protozoan parasite *Trypanosoma cruzi,* and leads to almost 10,000 deaths every year, affecting millions of people [1]. Globalization and the migratory flux of infected individuals to well-developed areas allowed the identification of Chagas disease cases in all continents [2,3]. The classical transmission involves the vector triatomine; however, due to successful control programs, new cases are mainly related to congenital or oral infections [4,5]. In Brazil, the presence of *T. cruzi* DNA has been frequently described in fruits such as açai and its products [6].

Regarding clinical manifestations, Chagas disease presents two very distinct phases: the acute phase, commonly asymptomatic and distinguished by high parasitemia in blood, and the chronic phase, characterized by the absence of parasites in the bloodstream. Additionally, after an asymptomatic period (indeterminate phase), chronic patients may present clinical manifestations, such as cardiac, digestive and/or neurological alterations [1,7,8].

In clinical use since the 1960s, benznidazole and nifurtimox are the only current options for Chagas disease treatment. Despite the high

* Corresponding author.
*E-mail addresses:* rubemsadok@gmail.com, rubemb@ioc.fiocruz.br (R.F.S. Menna-Barreto).
[1] These authors contributed equally to this work.
[2] In memoriam.

https://doi.org/10.1016/j.biopha.2020.111186
Received 9 October 2020; Received in revised form 16 December 2020; Accepted 26 December 2020
Available online 1 January 2021

activity in acute cases, low efficacy and serious adverse effects were observed during the treatment of chronic patients [9,10]. Their high toxicity and debatable activity during the chronic phase motivated the continuous multidisciplinary efforts for the development of preclinical and clinical trials of novel drugs (including natural products) and/or combinations [11].

Bioactive naphthoquinones, as lapachol (**1**) and β-lapachone (**2**), are isolated from the heartwood of *Tabebuia* sp. (bignoniaceae) and have effects on a large variety of pathogens, including protozoan parasites [12–14]. A series of β-lapachone derivatives were synthesized exploring the reactivity of their quinoidal carbonyls towards nucleophilic reagents and were screened on *T. cruzi* infective forms [15]. Among the most promising derivatives, naphthoimidazoles named N1, N2 and N3 (Fig. 1A) showed high trypanocidal activity and relatively low toxicity *in vitro* [16–18], encouraging our group to investigate their mechanism of action [19–25]. Active on all parasite stages, N1, N2 and N3 were more effective on trypomastigotes and amastigotes, the clinically relevant forms. Ultrastructural analysis pointed to the mitochondrion and autophagic pathway as the primary targets of these three naphthoimidazoles [23,25]. Subsequent studies, using proteomic and biochemical techniques, confirmed the central role of the mitochondria in the mode of action of N1, N2 and N3 in epimastigotes and bloodstream trypomastigotes [20,24], showing that the mitochondrial electron transport system (ETS) was severely affected by the treatment [19]. Unfortunately, our very recent work showed a discrete effect of these three naphthoimidazoles on acute infection in mice, leading to a partial reduction in parasitemia and no protective effect on mortality. However, N1 presented cardioprotective and immunomodulatory effects, deserving further analysis in this direction [21].

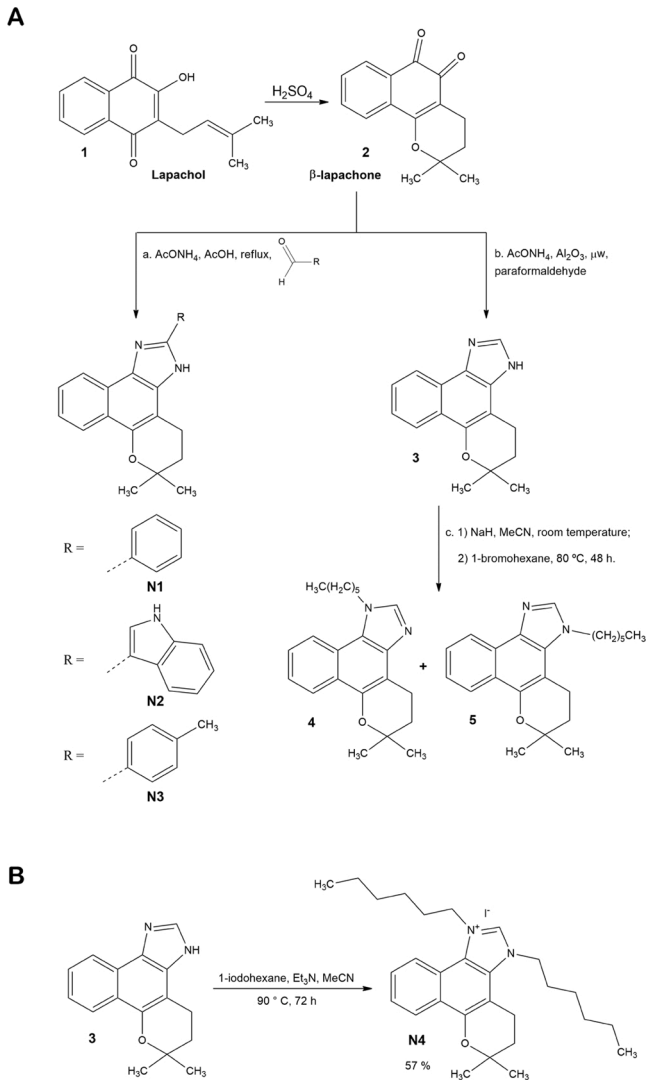


**Fig. 1. Chemical structures of β-lapachone and naphthoimidazoles. (A)** General procedure for obtaining β-lapachone and the derived naphthoimidazoles. The methods for synthesis were adapted from: a. [27]; b. [28]; c. [26]. Lapachol (1), β-lapachone (2), 6,6-dimethyl-3,4,5,6-tetrahydrobenzo[7,8]chromeno[5,6-*d*]imidazole (3), 1-hexyl-6,6-dimethyl-1,4,5,6-tetrahydrobenzo[7,8]chromeno[5,6-*d*]imidazole (4), 3-hexyl-6,6-dimethyl-3,4,5,6-tetrahydrobenzo[7,8]chromeno[5,6-*d*]imidazole (5). **(B)** Synthesis of N4 1, 3-dihexyl-6,6-dimethyl-3,4,5,6-tetrahydrobenzo[7,8]chromeno[5,6-*d*]imidazol-1-ium iodide).

In 2017, Silva and colleagues synthesized and studied a series of *N*-alkyl naphthoimidazoles by alkylation of compound **3**, a naphthoimidazole derived from β-lapachone. The *N*-alkyl-naphthoimidazoles **4** and **5** (Fig. 1A) demonstrated promising trypanocidal activity, being more effective than benznidazole in the same experimental conditions and having a selectivity index (SI) of 2.7 and 13.4, respectively [26]. Here, we show the synthesis of a novel β-lapachone-derived naphthoimidazolium by di-alkylation of compound **3** (Fig. 1B) and the assessment of its biological activity on *T. cruzi* stages.

## 2. Material and methods

### 2.1. Synthesis and characterization of N4

For the chemical characterization, all solvents used were of analytical grade. Column chromatography was performed using silica gel, 220–440 mesh particle size, 60 Å (Merck, Darmstadt, Germany). The $^{1}$H- and $^{13}$C-NMR spectra were recorded at room temperature using a Bruker Advance III (500 MHz) spectrometer, in deuterated dimethyl sulfoxide (DMSO-$d_6$), with tetramethylsilane (TMS) as the internal standard. Chemical shifts ($\delta$) are given in ppm and coupling constants ($J$) in hertz. High-resolution mass spectra were obtained using a Time of Flight (TOF) compact electrospray ionization instrument (Bruker Corporation, Billerica, USA) (Farmanguinhos, Fiocruz), with $N_2$ as the carrier gas. The main fragments were described as a relationship between the atomic mass units and the charge ($m/z$) and the relative abundance in percentage of the base peak intensity (see spectral data and Table S1 in supplementary material).

Lapachol was extracted from a sample of the pulverized heartwood of *Tabebuia* sp. obtained in the Seropédica region (RJ – BR) in June 2017, and converted to β-lapachone by the well-known method of isomerization into concentrated sulfuric acid [29]. Compound **3**, the precursor of N4, was obtained by the reaction between β-lapachone, paraformaldehyde and ammonium acetate supported on basic alumina in a domestic microwave oven, as previously described [28]. To obtain the compound N4, a mixture of 0.8 mmol of **3** (201.6 mg), 0.8 mmol of anhydrous triethylamine (56 μL), 20 mL of anhydrous acetonitrile and 3.2 mmol of 1-iodohexane (472 μL) was stirred at 90 °C for 72 h in a closed vial. Then, the acetonitrile was evaporated, and the sample was dissolved in ethyl acetate. Water was added, and partition gave an organic phase that was dried over anhydrous sodium sulfate. Column chromatography (1:3 hexane/ethyl acetate as eluent) was then performed on the concentrated organic layer.

### 2.2. Parasites, animals and host cells

The Y strain of *T. cruzi* was used for all experiments. Infected albino *Swiss* mice were euthanized at the peak of parasitemia, and bloodstream trypomastigotes were purified by differential centrifugation [30]. Axenic epimastigotes were maintained at 28 °C in liver infusion and tryptose (LIT) medium supplemented with 10 % fetal bovine serum (FBS) (Cultilab, Campinas, Brazil) and used for all experiments only at the exponential growth phase (5-day-old cultures) [31]. To assess intracellular forms of the parasite, peritoneal macrophages from

non-infected male Swiss mice (5–6 weeks) were obtained as previously described [32]. This work is in accordance with the guidelines of the Colégio Brasileiro de Experimentação Animal (COBEA) and was performed in biosafety conditions. All animal procedures were reviewed and approved by the Fiocruz Committee of Ethics in Animal Research (L-005/2017) according to resolution 196/96 of the National Health Council of Brazilian Ministry of Health.

### 2.3. Direct effect analysis

A solution (100 µL) of bloodstream trypomastigotes ($1 \times 10^7$ parasites/mL) resuspended in RPMI medium (Sigma-Aldrich, St. Louis, USA) containing 10 % FBS and 10 % mouse blood was added to the same volume of N4 at twice the desired final dose and incubated in 96-well microplates (Nunc Inc., Rochester, USA) at 4 °C for 24 h. Alternatively, the assays were also performed in the absence of blood at 37 °C. The experiments with epimastigotes were performed in LIT at 28 °C for 24 h. After the incubation time, the quantification was performed using the Neubauer chamber, and the activity of the compounds was expressed as $IC_{50}$/24 h, corresponding to the concentration that leads to 50 % parasite lysis. An N4 stock solution was prepared in dimethylsulfoxide (DMSO, Merck, Darmstadt, Germany), and the solvent final concentration never exceeded 0.1 %, with no deleterious effect on *T. cruzi* [33].

### 2.4. Effect on amastigotes and mammalian toxicity analysis

Peritoneal macrophages ($3 \times 10^5$ cells/well) plated in 24-well plates (Nunc Inc.) were infected with bloodstream trypomastigotes (10 parasites/host cell) for 24 h. Then, the cultures were washed in phosphate buffered saline (PBS, pH 7.4, Sigma-Aldrich) to remove non-internalized parasites, and N4 (0.5–2.0 µM) was added for 24 h at 37 °C. After this period, the cells were fixed and stained with Panotic dye kit (Laborclin, Rio de Janeiro, Brazil), and the parameters of percentage of infection, parasites per cell and infection index (percentage of infected host cells multiplied by the number of parasites per cell) were calculated after the quantification of 300 cells per coverslip using Zeiss Axioplan microscope (Oberkochen, Germany) [34].

In parallel, uninfected macrophages ($5 \times 10^4$ cells/well) were employed to evaluate the toxicity of N4 to the host cells. After 24 h treatment at 37 °C, 10 µL PrestoBlue (Invitrogen, Carlsbad, USA) was added to the cells (final concentration of 10 %) for 2 h, and the data acquired at 560 and 590 nm in SpectraMax M3 Microplate Reader (Molecular Devices, San Jose, USA). These results were expressed as $LC_{50}$/24 h, which corresponds to the concentration that leads to a damage of 50 % in macrophages, and SI was calculated by the ratio of $LC_{50}$/24 h (uninfected macrophages) and $IC_{50}$/24 h (infection index parameter).

### 2.5. Ultrastructural analysis

Epimastigotes ($5 \times 10^7$ parasites/mL) were treated with 1.2 and 2.4 µM N4 in LIT medium at 28 °C for 24 h. After this period, control and treated parasites were fixed with 2.5 % glutaraldehyde (Sigma-Aldrich) diluted in 0.1 M Na-cacodylate buffer (pH 7.2) for 40 min and post fixed with 1 % osmium tetroxide (Sigma-Aldrich) diluted in the same buffer, adding 2.5 mM calcium chloride and 0.8 % potassium ferricyanide for 20 min, both at 25 °C. After the washings, dehydration was performed in acetone (50, 70, 90 and 100 %) before embedding in PolyBed 812 (Polysciences Inc., Warrington, USA) resin for 72 h. Ultrathin sections were obtained and stained with uranyl acetate and lead citrate for the examination with a JEM1011 transmission electron microscope (Jeol, Tokyo, Japan). Alternatively, fixed epimastigotes were dehydrated in ethanol (50, 70, 90 and 100 %), dried by the critical point method with $CO_2$, mounted on aluminum stubs, coated with a 20-nm-thick gold layer, and analyzed with a Jeol JSM6390LV scanning electron microscope. Both electron microscopes are located in Plataforma de Microscopia Eletrônica Rudolf Barth (Instituto Oswaldo Cruz, Fiocruz).

### 2.6. Flow cytometry analysis

Epimastigotes ($5 \times 10^6$ parasites/mL) were treated with 1.2 and 2.4 µM N4 for 24 h, washed with PBS, and labeled with 32 ng/mL rhodamine 123 (Rh123) and 10 µg/mL propidium iodide (PI) (Sigma-Aldrich) for 30 min to assess mitochondrial membrane potential ($\Delta\Psi m$) and plasma membrane integrity, respectively. As positive controls, parasites were preincubated with 10 µM carbonyl cyanide 4-(trifluoromethoxy) phenylhydrazone (FCCP, Sigma-Aldrich) or 0.1 % saponin (Sigma-Aldrich) for 30 min at 28 °C. All Rh123 data were normalized by the addition of FCCP at each experimental condition. Rh123 fluorescence was monitored by variation index (VI), which corresponds to the equation (MT - MC)/MC, with MT being the fluorescence median of treated parasites and MC the fluorescence median of untreated parasites. Negative VI values represent the mitochondrial membrane depolarization. All data were acquired with a FACSCalibur flow cytometer (Becton Dickinson, Franklin Lakes, USA) equipped with Cell Quest software (Joseph Trotter, Scripps Research Institute, La Jolla, USA), totaling 10,000 events in the region previously established to correspond to epimastigotes. The analyses were performed using the Summit 6.1 software (Beckman Coulter, Brea, USA).

### 2.7. High resolution oxygraphy and ATP production analysis

Epimastigotes ($1 \times 10^7$ parasites/mL) were treated with 1.2 and 2.4 µM N4 for 24 h and washed with PBS. Then, $5 \times 10^7$ parasites were resuspended in 2 mL of respiration buffer (125 mM sucrose, 5 mM succinate, 65 mM potassium chloride, 10 mM Tris-HCl pH 7.2, 1 mM magnesium chloride, and 2.5 mM monobasic potassium phosphate) to evaluate the $O_2$ flux and concentration. The analysis was made in a high resolution respirometry 2 K (Oroboros Instruments, Innsbruck, Austria) at 28 °C and under continuous stirring. The data were acquired by DatLab 5.1 software, and the addition of 2 µM antimycin A (AA) was used to assess residual oxygen consumption (ROX), as previously reported [30]. For ATP analysis, $1 \times 10^8$ parasites were resuspended in 100 µL PBS, added to the same volume of luminescent reagent CellTiter-Glo Luminescent Cell Viability Assay (Promega, Madison, USA) in 96-well microplates (Nunc Inc.) and incubated for 15 min at room temperature. The bioluminescence was measured according to manufacturer's instructions in a SpectraMax M3 Microplate Reader (Molecular Devices) and a standard curve was made with ATP.

### 2.8. Biochemical analysis

Epimastigotes ($1 \times 10^7$ parasites/mL) were treated with 1.2 and 2.4 µM N4 for 2, 4 and 24 h, washed with PBS and thawed. After that, the protozoa were disrupted by sonication, as previously described [35]. Protein concentration was determined using the Pierce™ BCA Protein Assay Kit (Thermo Fisher, Waltham, EUA) in the soluble fraction (16, 000 g for 10 min). Alternatively, epimastigotes were pre-treated with 10 nM MitoTEMPO (Santa Cruz Biotechnology, Dallas, Texas, USA) for 30 min in the same conditions previously described and treated for another 2 or 4 h with 1.2 and 2.4 µM N4. The AA-sensitive succinate: cytochrome c oxidoreductase activity (complexes II–III) is based in ferrocytochrome c reduction at 550 nm ($\varepsilon$ =19 $mM^{-1}$ $cm^{-1}$) and was measured in a reaction mixture consisted of 100 mM potassium phosphate buffer (pH 7.4), 150 µM bovine heart cytochrome c, 3 mM succinic acid and 1 mM KCN. The measurement of KCN-sensitive cytochrome c oxidase (complex IV) activity is based on the ferrocytochrome c oxidation at 550 nm ($\varepsilon$ =19 $mM^{-1}$ $cm^{-1}$) and the reaction mixture consisted of 100 mM potassium phosphate buffer pH 7.4 and 50 µM sodium dithionite reduced equine heart cytochrome c. In both assays, the reactions started with the addition of 0.5 mg/mL, and specific controls were made with 2 µM AA or 1 mM KCN to complexes II-III and IV,

respectively [19]. To assess trypanothione reductase (TR) activity, the samples (0.25 mg/mL) were added to 1 μM $T(SH)_2$, 150 μM NADPH, 400 mM HEPES pH 7.5, 25 μM DTNB and 1 mM EDTA, and 2TNB production was measured at 412 nm [36]. Mitochondrial complexes and TR activities were analyzed at room temperature in a total reaction volume of 200 μL in SpectraMax M3 Microplate Reader (Molecular Devices).

### 2.9. Hydrogen peroxide release analysis

Epimastigotes ($1 \times 10^7$ parasites/mL) were treated with 1.2 and 2.4 μM N4 for 2, 4 and 24 h, washed with PBS and incubated with 5 μM Amplex Red and 200 μg/mL HRP in respiration buffer [37]. Resorufin production was evaluated at 530 and 590 nm in SpectraMaxM3 Microplate Reader (Molecular Devices). Menadione (4 μM) was added as a positive control 2 h before reagent addition, and the pretreatment with 10 nM mitoTEMPO was performed together with the treatment for 2 and 4 h with N4. A standard curve was made with hydrogen peroxide ($H_2O_2$, Merck), and the assay was carried out in a total volume of 200 μL with $1 \times 10^8$ parasites per well.

### 2.10. Molecular docking procedure

The chemical structure of the naphthoimidazolium N4 was built and energy-minimized by Density Functional Theory (DFT), with the Becke-3-Lee Yang Parr (B3LYP) method and standard 6-31G* basis set, available in Spartan'18 software (Wavefunction, Inc., Irvine, USA) (https://www.wavefun.com/). The crystallographic structure for dihydroorotate dehydrogenase (DHODH) from the *T. cruzi* Y strain was obtained from the Protein Data Bank (PDB - https://www.rcsb.org/) with access code 2E6D [38]. Because the 3D structure of succinate dehydrogenase (complex II) from *T. cruzi* is not still available, a model was built from the corresponding protein sequence of this parasite available in UniProt (https://www.uniprot.org/). The Swiss Model software (University of Basel, Basel, Switzerland) (https://swissmodel.expasy.org/) was applied to the search set to select the template structures for comparative modeling and construct the protein model with the highest reliability. Fifty models were generated with the standard 'auto model' routine of Swiss Model, and the best resulting modeled structure was chosen according to the QMEAN value.

Molecular docking was performed with GOLD 5.7 software (Cambridge Crystallographic Data Centre, Cambridge, UK) (https://www.ccdc.cam.ac.uk/solutions/csd-discovery/components/gold/). Hydrogen atoms were added to the biomacromolecules according to the data inferred by GOLD 5.7 software on the ionization and tautomeric states. Redocking studies with the crystallographic cofactor flavin mononucleotide (FMN) in the DHODH structure [38] were carried out to define the best scoring function. The obtained root mean square deviation (RMSD) value for *ChemPLP*, *Goldscore*, *ChemScore* and *ASP* was 0.4545, 0.9823, 1.7418, and 1.4757, respectively, indicating the standard *ChemPLP* as the best scoring function to simulate N4 in the proteins. A 10 Å radius spherical cavity around FMN and flavin adenine dinucleotide (FAD) for DHODH and complex II, respectively, was selected, and docking studies with N4 (*ChemPLP*) were carried out. In addition, the ubiquinone site of succinate dehydrogenase was also explored. The figures for the docking poses of the largest docking score value were generated with PyMOL Delano Scientific LLC software (Schrödinger, New York, USA) (https://www.pymol.org/2/).

### 2.11. Statistical analysis

A nonparametric Mann-Whitney test with IBM SPSS Statistics 22.0 software (IBM Corporation, New York, USA) was employed with the threshold for significance set at $p \leq 0.05$. The pairwise comparisons are described in the respective figure legends.

## 3. Results

The method applied to the alkylation of compound **3** produced 250 mg of the dialkylated naphthoimidazolium named N4 (57 % yield). Chemical structures of β-lapachone and its derivative N4 were displayed in Fig. 1B (See spectral data and Table S1 in supplementary material). Treatment with N4 was effective against bloodstream trypomastigotes, intracellular amastigotes and epimastigotes with $IC_{50}$/24 h ranging from 0.8 to 7.9 μM (Table 1). On bloodstream forms, N4 was 10-fold less active at 4 °C in the presence of 5% blood than at 37 °C in the absence of blood. Cytotoxicity analysis pointed to an adverse effect of the compound on murine macrophages ($LC_{50}$/24 h = 4.3 ± 0.1 μM), and consequently SI = 5.4 (Table 1).

To investigate the mechanism of action, we selected the axenic proliferative form epimastigote and the concentrations of 2.4 and 1.2 μM, which correspond to $IC_{50}$/24 h and half of it, to continue the experiments. Scanning electron microscopy (SEM) analysis evidenced normal morphological aspect of untreated epimastigotes, presenting the typical elongated body (Fig. 2A, B), and important shape alterations, such as body torsion and retraction, as well as spherical aspect and bleb formation in the flagellar membrane of N4-treated parasites (2.4 μM) (Fig. 2C–F). Abnormal morphology was also detected in epimastigotes during cytokinesis (Fig. 2F). No important alteration was detected in epimastigotes treated with 1.2 μM N4 by scanning electron microscopy (data not shown). In transmission electron microscopy (TEM), classical morphological features of subcellular structures and organelles were observed in untreated parasites (Fig. 3A,B). Epimastigotes treated with 2.4 μM N4 presented a notable mitochondrial swelling, with washed out aspect of its matrix, intense loss of cristae and the presence of concentric membrane structures (Fig. 3C–F). The treatment also induced the blebbing formation in the parasite flagellum (Fig. 3D, inset), as well as the appearance of epimastigotes with two kinetoplasts or nuclei (Fig. 3E, F). TEM analysis of parasites treated with 1.2 μM N4 showed similar swelling phenotype on the mitochondrion; however, smaller washed out aspects could be observed (Fig. S1).

Once mitochondria appeared to be the main target of N4 treatment, the functionality of this organelle was assessed by oxygen consumption, ΔΨm and complex activities analysis. Both N4 concentrations (1.2 and 2.4 μM) severely impaired oxygen uptake in the routine stage (reduction of 45–48%), although no dose-dependent effect was detected. AA was employed to reach the ROX stage, reinforcing the mitochondrial oxygen consumption. Curiously, the ROX stage was 49 % less in parasites treated with 2.4 μM N4 than in untreated parasites (Figs. 4A and S2). The treatment with N4 also affects the mitochondrial complexes activities. Both tested concentrations similarly decreased the activity of mitochondrial complexes II-III (reduction of 37.5–48.2%) (Fig. 4B). Interestingly, complex IV activity and ATP production were only affected after the treatment with the highest concentration, with a loss of 48.7 % in enzymatic activity and 75.6 % in energy production (Fig. 4C, D). Flow cytometry analysis showed a decrease of 53 % in ΔΨm of parasites treated with 2.4 μM N4; however, there was no effect of the treatment with the lowest concentration (Table 2 and Fig. S3). FCCP was

**Table 1**
Effect of N4 on all *T. cruzi* stages.

| Parasite stage | Experimental condition | $IC_{50}$/24 h | SI |
|---|---|---|---|
| Trypomastigotes | 4 °C, 5% blood | 7.9 (± 0.7)[a] | ND[b] |
| Trypomastigotes | 37 °C, 0% blood | 0.8 (± 0.1) | ND |
| Intracellular amastigotes[c] | 37 °C, macrophages | 0.8 (± 0.04)[c] | 5.4[d] |
| Epimastigotes | 28 °C, LIT medium | 2.4 (± 0.2) | ND |

[a] Mean ± SD of at least three independent experiments.
[b] Not determined.
[c] Based on infection index.
[d] Selectivity Index (SI) = $LC_{50}$/24 h in peritoneal macrophages / $IC_{50}$/24 h in intracellular amastigotes.

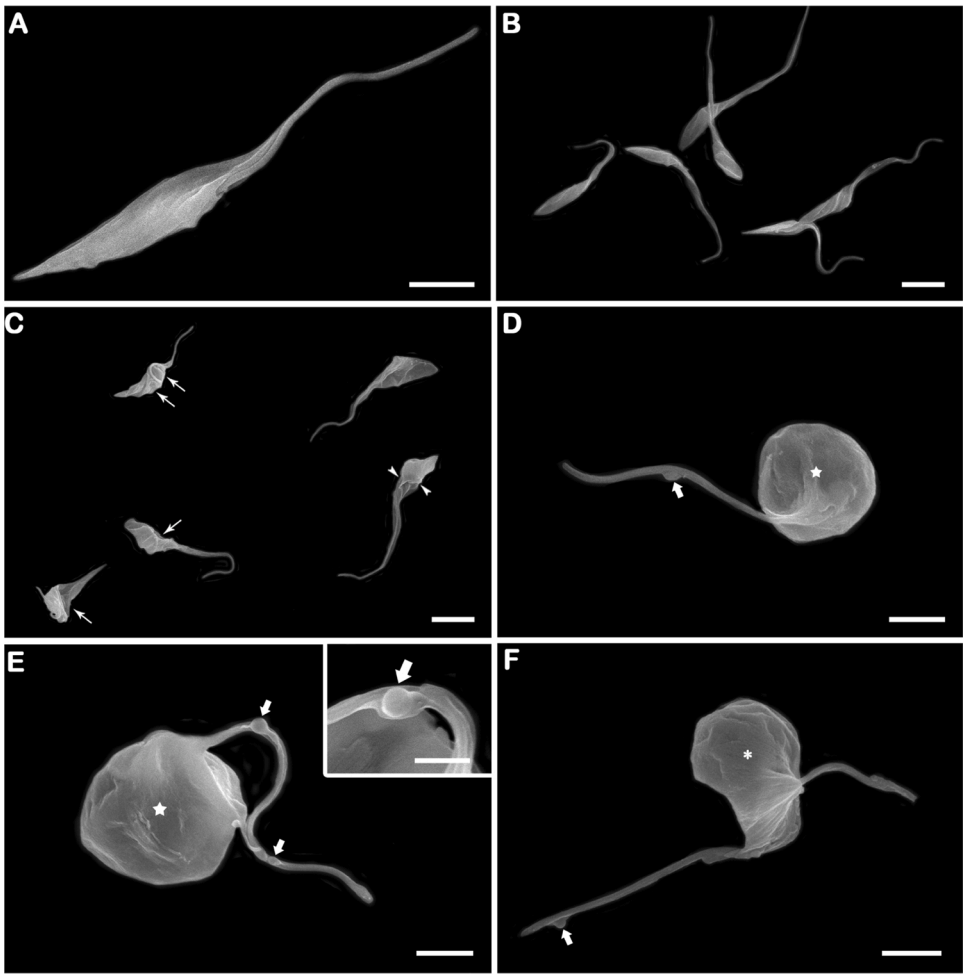


**Fig. 2. SEM analysis of *T. cruzi* treated epimastigotes.** (**A,B**) Untreated parasites showed typical elongated bodies. (**C-F**) The treatment with 2.4 μM N4 for 24 h led to the protozoa body torsion (white arrows) and retraction (white arrowheads), frequently showing a spherical appearance and blebs in the flagellar region (white thick arrows). (**F**) Remarkable shape alterations were also observed in epimastigotes during cytokinesis (white asterisk). Bars in A, D and F =2 μm; Bars in B, C and E =5 μm; Bar in inset E =1 μm.

added in each condition to ensure the measure of ΔΨm. The treatment with the naphthoimidazolium did not induce plasma membrane permeabilization (Table 2).

The main consequence of mitochondrial impairment is reactive oxygen stress (ROS) imbalance [39]. Epimastigotes submitted to 1.2 μM N4 do not show alterations in $H_2O_2$ production compared to untreated parasites; however, the treatment with 2.4 μM decreased by 76 % the reactive species production (Fig. 5A). Additionally, biochemical analysis showed that the treatment with both concentrations of N4 increased the TR activity 65.3 and 226.2 % (Fig. 5B). To confirm that ROS generation does not participate in the mechanism of action of this naphthoimidazolium, we tested the concentrations of 1.2 and 2.4 μM for shorter treatment times (2 and 4 h) alone and together with 10 nM mitoTEMPO. After 2 h, the treatments with 1.2 and 2.4 μM increased $H_2O_2$ production by 26.2 and 72.3 %, respectively. ROS production in N4 treated parasites appears to be time-dependent, as the treatment for 4 h increased the difference to 112.4 and 425.6 % in comparison to the untreated control. Corroborating our previous data, $H_2O_2$ generation was mitochondrial and decreased in the presence of 10 nM mitoTEMPO (Fig. 6A, B). We also evaluated the TR activity in short treatment times. Although at 2 h it was not possible to observe differences between the untreated and N4-treated groups, we observed upregulation (54.6–167.7%) of this antioxidant enzyme after 4 h (Fig. 6C, D). To determine if ROS production was the cause or consequence of the mitochondrial damage seen previously, we evaluated the activity of its enzyme complexes. Fig. 6E and F show that complexes II-III were affected early and had a reduction in the range of 31.5–49.0% of its activity. Additionally, the antioxidant presence influenced the enzyme activity only at 4 h, protecting complexes II-III functionality. These phenotypes were not observed for complex IV, which does not appear to be affected by short treatment times with N4 (Fig. S4).

Because experimental data clearly indicated that N4 can interfere in mitochondrial physiology, molecular docking calculations were carried out to evaluate if the compound has a direct effect on succinate dehydrogenase. First, we choose the FAD and ubiquinone binding sites to test N4 action. The highest molecular docking score values for N4 in the FAD and ubiquinone sites were 58.2 and 74.2 (dimensionless), respectively (Fig. 7A). These data suggest that N4 could interact mainly in the ubiquinone binding site in mitochondrial complex II *via* van der Waals forces with the amino acid residues Ile-30, Met-39, Ile-43, Tyr-91, Arg-93, Pro-169, Trp-173, and Ile-218 with a distance of 3.50, 2.30, 3.50, 1.70, 3.00, 3.40, 2.90, and 2.40 Å, respectively. Because succinate is the main energetic substrate for ETS in trypanosomatids [40,41], we also analyzed the effect of N4 in DHODH. The score of the FAD binding site of DHODH was 71.4 (Fig. 7B), suggesting that N4 could also interfere with the biological action of this enzyme by the interaction with six of the key amino acid residues that are responsible for the interaction with the substrate fumarate (Lys-43, Met-69, Leu-71, Asn-127, Asn-132, and Asn-194 residues). In the three analyzed sites, the interactions between N4 and amino acid residues were mainly by van der Waals forces; however, hydrogen bonding also occurs in some cases (Table S2).

## 4. Discussion

Natural naphthoquinones, such as lapachol, β-lapachone and lawsone, are isolated from vegetal sources, and their biological activity has

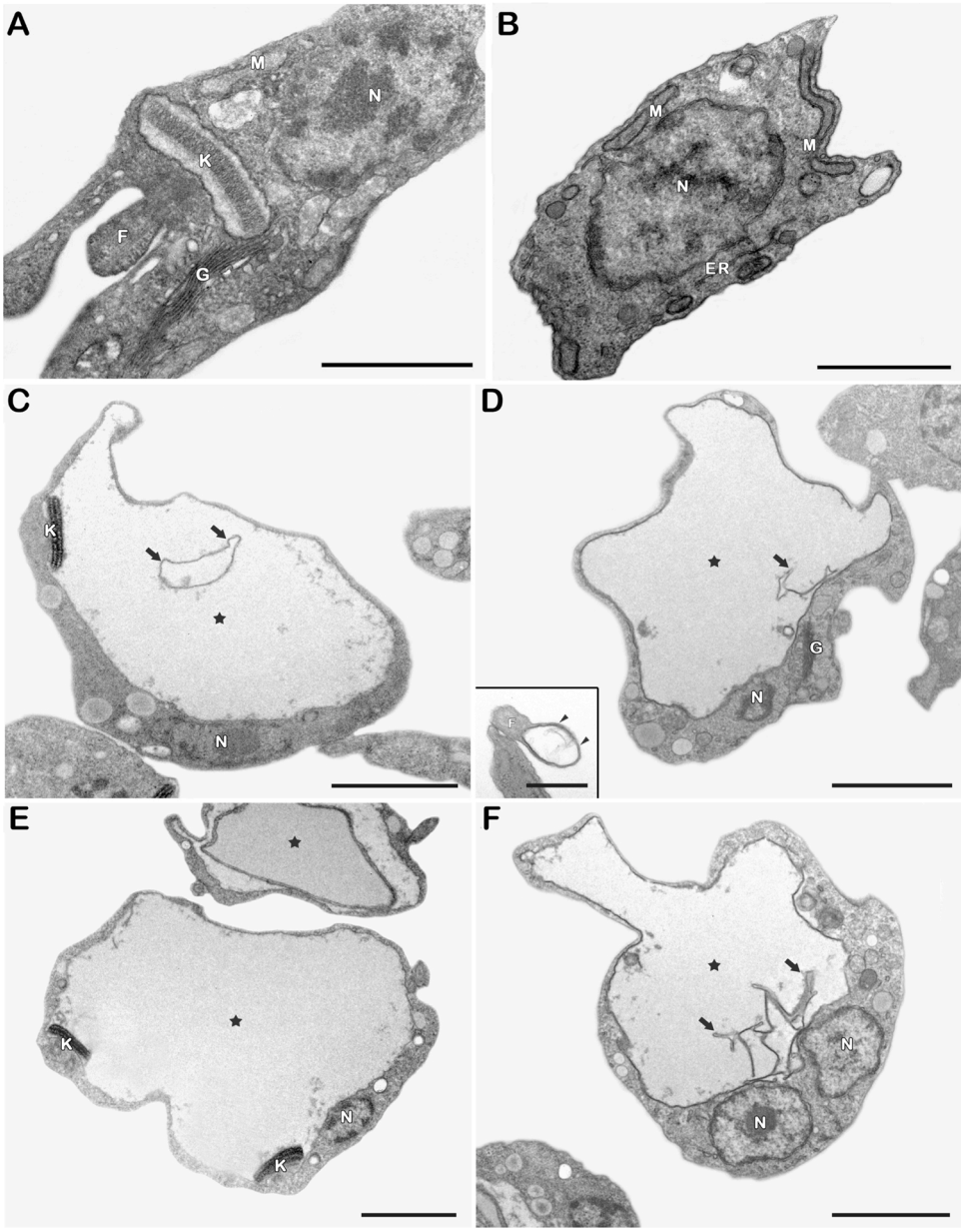


**Fig. 3. TEM analysis of *T. cruzi* epimastigotes treated with N4. (A,B)** Untreated parasites showed typical morphological characteristics. (**C-F**) The treatment with 2.4 μM N4 for 24 h induced a strong mitochondrial swelling (black stars), with concentric membrane structures inside this organelle commonly observed (black arrows). In detail, blebs in the flagellar membrane (black arrowheads). Parasites presenting two kinetoplasts (**C**) or two nuclei (**D**) were also detected after the treatment. Nucleus (N), kinetoplast (K), mitochondrion (M), Golgi (G), endoplasmic reticulum (ER) and flagellum (F). Bars in A, B =1 μm. Bars in C-F =2 μm; Bar in inset D =0.5 μm.

been described [15,42]. Related quinones are based on series of recrystalizations. In lapachol, sulfuric acid induces the nucleophylic attack of oxygen on the isoprenyl lateral chain cyclization, resulting in β-lapachone [43]. In another step, aromatic aldehydes react with β-lapachone in the presence of ammonium acetate, generating naphthoimidazoles as product [16–18,26]. The biological effects of naphthoimidazoles were demonstrated in many organisms, in which antibacterial and anti-inflammatory activities were present [44–47]. Since the first report about the trypanocidal activity of β-lapachone *in vitro* in the late 1970s, many series of derivatives were synthesized and assayed against *T. cruzi* [15].

In a previous study of our group, Silva et al. [26] investigated the correlation between trypanocidal activity and the chemical structure of *N*-alkyl and aryl-naphthoimidazoles derived from β-lapachone, pointing out the alkyl substitution on the imidazole ring as an important factor for the trypanocidal activity. In this work, naphthoimidazoles **4** and **5** were tested on infective forms of the parasite and showed moderate efficacy and selectivity, being 2.2 and 3.2-fold more active than the standard drug benznidazole [26]. Continuing these studies, the substitution of 1-bromohexane and sodium hydride, used in the synthesis of compounds **4** and **5**, by 1-iodohexane and triethylamine, respectively, enabled the synthesis of a novel di-alkylated naphthoimidazolium, N4. One possible explanation for the difference observed between the results of the single and double alkylation methods is the fact that iodide is a better leaving group than bromide in nucleophilic substitution reactions. Use of a weaker base is also favorable due to the possibility of competition between the nucleophilic substitution reaction and the elimination reaction.

The comparison between the trypanocidal effects of N4 and N1, N2 and N3 *in vitro* showed that the new naphthoimidazolium is most active on all parasite stages. On bloodstream forms, N4 was 2.0–4.7-fold and 15.4–44.8-fold more effective at 4 °C in 5% blood or 37 °C in 0% blood, respectively [16–18,23,25]. Such increased activity was also detected on proliferative forms of the parasite, in the range of 12.8–34.2-fold on epimastigotes and 11.3–15.5-fold on intracellular amastigotes [23,25]. Until now, N1, N2 and N3 were the most active naphthoimidazoles tested on *T. cruzi in vitro*, but their moderate trypanocidal effect in an acute murine model and their high toxicity *in vivo* pointed out the

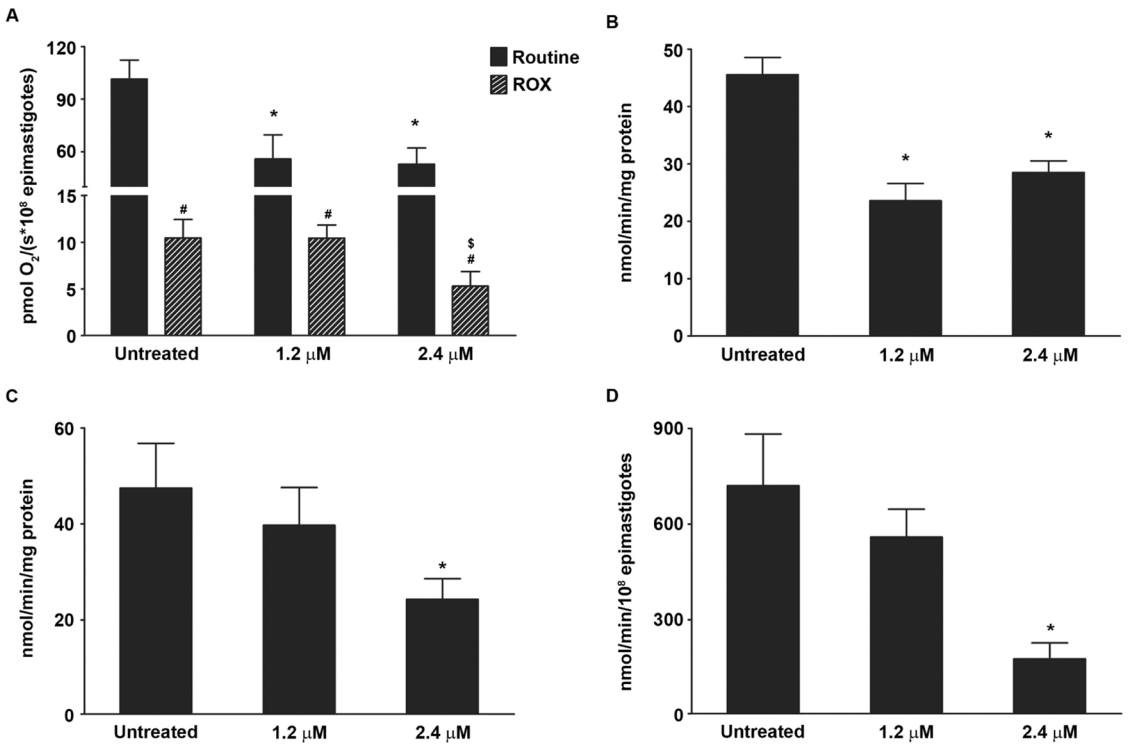


**Fig. 4. Mitochondrial metabolism analysis in *T. cruzi* treated epimastigotes.** (**A**) The treatment with 1.2 and 2.4 μM N4 for 24 h induced an important reduction in the parasite $O_2$ consumption during routine stage (open bars). AA (2 μM) was added (ROX state) to confirm that $O_2$ uptake was mitochondrial (dashed bars). (**B**) Both treatments also decreased complexes II-III activity in epimastigotes, while only 2.4 μM N4 for 24 h impaired complex IV activity (**C**) and ATP production (**D**). The graphs show means and standard deviations of at least three independent experiments. Significant differences in relation to the untreated group ($^{*}p \leq 0.05$). Significant differences in relation to the ROX untreated group ($^{\$}p \leq 0.05$). Significant differences comparing the routine and ROX of the same experimental group ($^{\#}p \leq 0.05$).

**Table 2**
Flow cytometry evaluation of ΔΨm and plasma membrane integrity of *T. cruzi* epimastigotes.

| | Rh123 median | IV Rh123 | % PI + parasites |
|---|---|---|---|
| Control | 451.3 ± 129.9[a,b] | 0.00[c] | 2.1 ± 0.6 |
| control + saponin | ND [d] | ND | 94.1 ± 2.8 |
| 1.2 μM N4 | 473.4 ± 187.9 | 0.05 [c] | 1.4 ± 0.4 |
| 2.4 μM N4 | 208.4[*] ± 48.3 | −0.53 | 1.8 ± 0.3 |

[a] Mean ± SD of at least three independent experiments.
[b] Rh123 labeling was ensured by the addition of 10 μM FCCP in each experimental condition.
[c] IV = (MT - MC)/MC, where MT is the median of fluorescence for treated parasites and MC is the median of fluorescence of the untreated parasites.
[d] Not determined.
[*] Significant differences to untreated parasites ($p \leq 0.032$).

necessity of optimization of the therapeutic project and alternative formulations [21]. Our results with N4 corroborate a tendency, shown in the series of compounds **4** and **5** [26], that the alkyl substitution increases activity up to a certain point (in this case n = 6–8 and is detrimental for longer chains). The van der Walls interactions with the plasmatic membrane (or minor groove of DNA) of the parasite would be favored by long alkyl chains. Too long of an alkyl chain could also sterically interfere with docking at the active site of the target enzyme [48–50].

Morphological and metabolic peculiarities accredit the unique mitochondria of trypanosomatids as an attractive target to chemotherapeutic strategies [51]. Quinones, such as β-lapachone, are easily reduced due to their high redox potential and have the biological activity commonly associated with their electrochemical behavior. Previous reports demonstrated that β-lapachone promoted a strong reduction in respiratory rates and mitochondrial swelling in *T. cruzi* epimastigotes, increasing the production of mitochondrial ROS [52–54]. In last fifteen years, our group made many efforts to understand of the mechanism of action of naphthoimidazoles on *T. cruzi*. Ultrastructural, proteomic and biochemical approaches indicated the central role of parasite mitochondria for the trypanocidal effect of N1, N2 and N3 [19,23–25]. In contrast to the data observed for the other three naphthoimidazoles, reservosome disorganization, Golgi disruption, alterations in genomic and/or kinetoplast DNA (condensation or fragmentation) and autophagic pathway triggering [23,25,55] were not detected after treatment with N4. On the other hand, mitochondrial swelling was more prominent at both tested concentrations and strongly suggests metabolic dysfunction. This hypothesis was confirmed by decreased respiratory rates and complex activities, as well as ΔΨm and ATP production. Our previous data showed similar metabolic dysfunction in epimastigotes treated with naphthoimidazoles and with naphthofuranquinones derived from C-allyl lawsone [19,38]. The mitochondrial metabolism was also confirmed as a primary target of N1, N2 and N3 by proteomic data, which evidenced the great number of mitochondrial proteins differentially expressed in treated epimastigotes and trypomastigotes [20,24].

Surprisingly, the assessment of ROS production showed that the treatment with N4 does not increase $H_2O_2$ release. In our previous work, we demonstrated that redox imbalance participated in N1, N2 and N3 trypanocidal mechanism. Additionally, the pretreatment with mito-TEMPO, a mitochondria-targeted antioxidant with superoxide and alkyl radical scavenging properties, decreased ROS production by N2 and N3 and improved mitochondrial physiology in all treated parasites [19]. Despite the differences in oxidative burst after 24 h, N4-treated epimastigotes have a similar antioxidant profile when compared to the other naphthoimidazoles. In both cases, the antioxidant system was triggered [24], which may be responsible for the low ROS release once

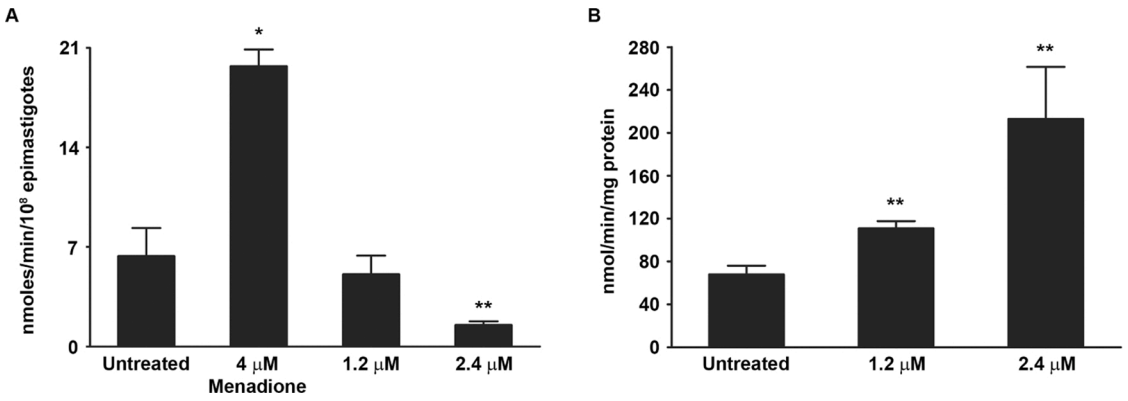


**Fig. 5. $H_2O_2$ release and TR activity in *T. cruzi* treated epimastigotes.** (**A**) The treatment with both N4 concentrations for 24 h does not induce ROS production. Menadione (4 μM) was used as a positive control. (**B**) N4 promoted an increase in TR activity after the treatment for 24 h in epimastigotes. The graphs show means and standard deviations of at least three independent experiments. Significant differences in relation to the untreated group (*$p \leq 0.05$; **$p \leq 0.03$).

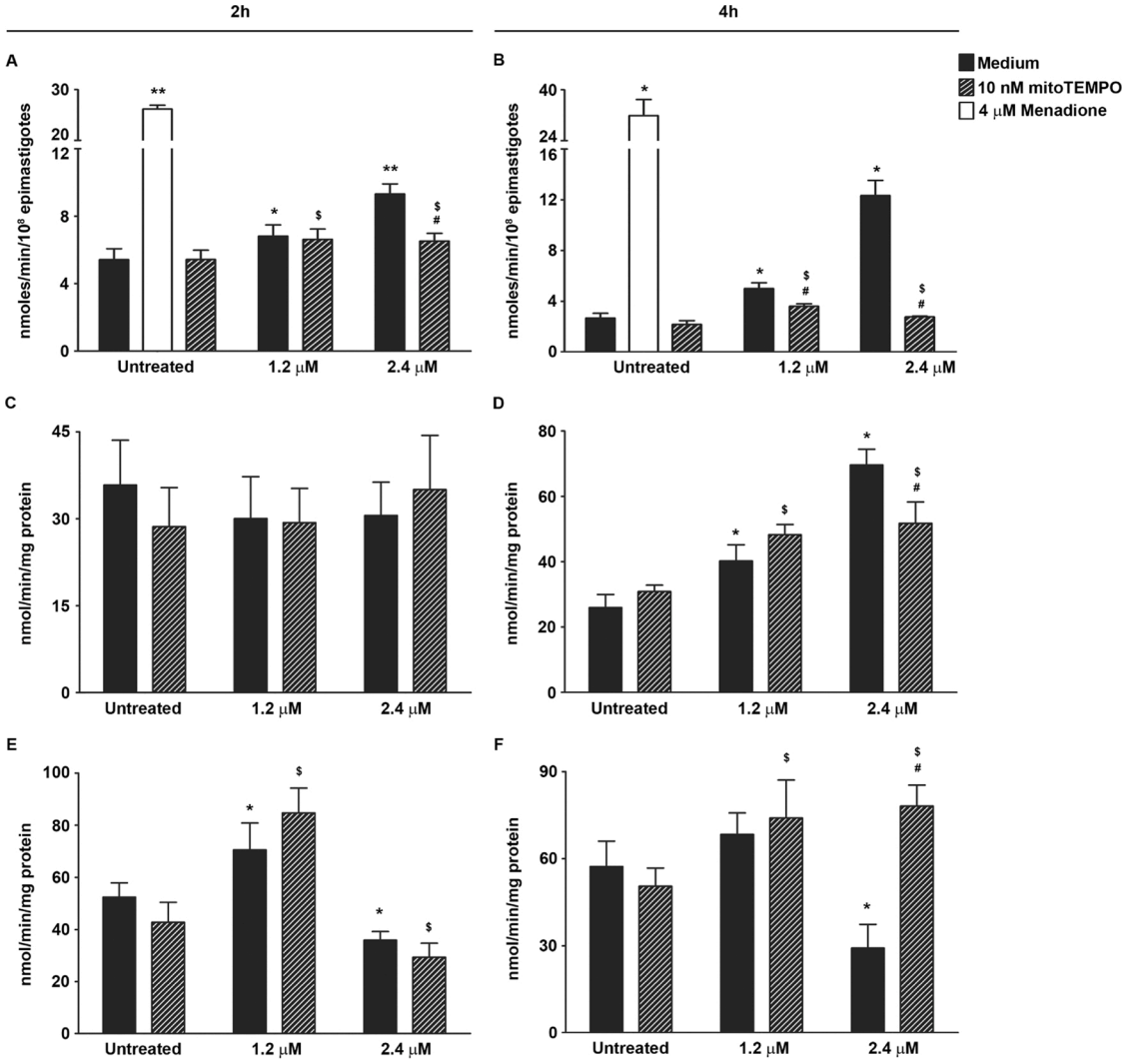


**Fig. 6. Redox metabolism and complexes II-III analysis in *T. cruzi* treated epimastigotes.** (**A**, **B**) The treatment with both N4 concentrations for 2 and 4 h increased ROS production in epimastigotes. The pretreatment with 10 nM mitoTEMPO partially reversed $H_2O_2$ production. Menadione (4 μM) was used as a positive control. (**C**, **D**) N4 promoted an increase in TR activity after the treatment for 4 h in epimastigotes. (**E**, **F**) The treatment with 2.4 μM decreased complexes II-III activity in both evaluated times. The antioxidant presence protected these mitochondrial complexes from damage in 4 h. The graphs show means and standard deviations of at least three independent experiments. Significant differences in relation to the untreated group (*$p \leq 0.05$; *$p \leq 0.05$). Significant differences in relation to the untreated group + mitoTEMPO ($^{\$}p \leq 0.05$). Significant differences comparing the same experimental group in the conditions with and without antioxidant ($^{\#}p \leq 0.05$).

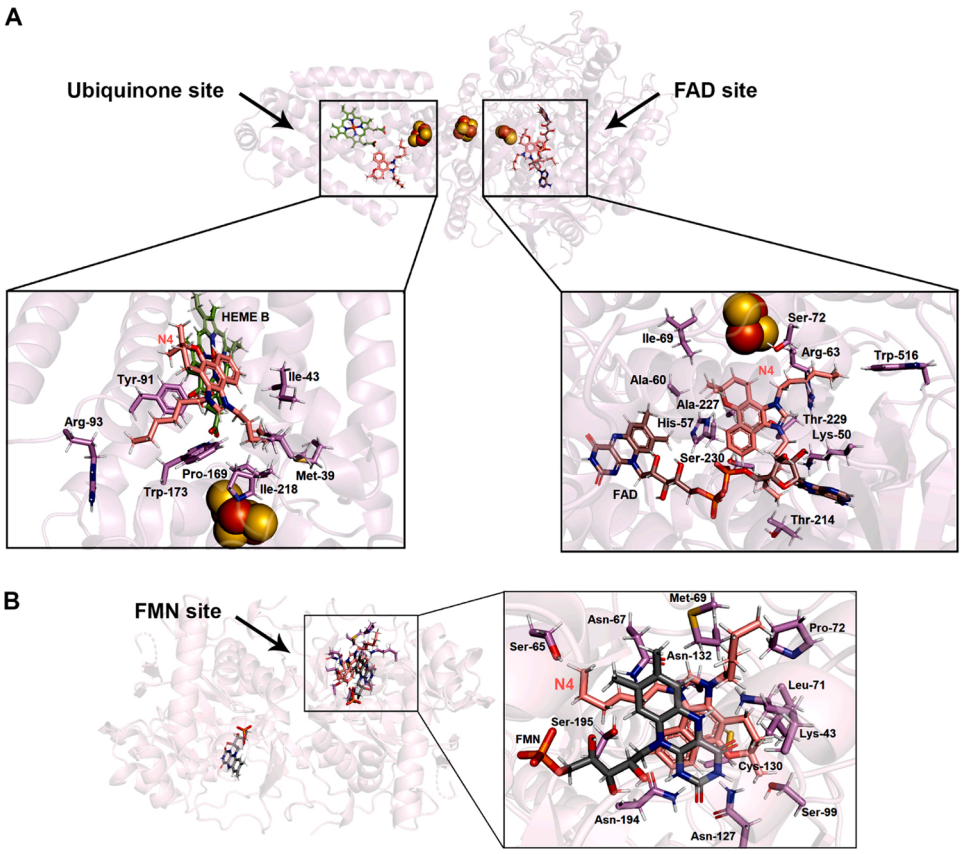


**Fig. 7. Molecular docking analysis for N4 in *T. cruzi* enzymes.** Interaction between N4 and (**A**) succinate dehydrogenase (uniquinone and FAD sites) or (**B**) DHODH (FMN site). For each protein site, the zoom representation shows the main amino acid residues which are interacting with the naphthoimidazolium under study. Selected amino acid residues, N4, FMN, FAD, and HEME are in stick representation in violet, beige, gray, brown, and green, respectively. Spheres are [Fe-S] complexes. Hydrogen, oxygen, nitrogen, sulfur, and phosphorus are in white, red, blue, yellow, and orange, respectively (For interpretation of the references to colour in this figure legend, the reader is referred to the web version of this article).

the oxidant environment is in a balance between pro-oxidant and antioxidant molecules [56]. To answer the question if ROS were generated at any point in the treatment, we decreased the exposure time to N4, aiming to observe the primary effect of the naphthoimidazolium. This strategy allowed us to demonstrate that reactive species production occurs as a consequence of N4 treatment in mitochondria and can be the main cause of the observed injuries. These data also highlighted oxidative stress control at 24 h as a parasite survival strategy. In comparison with N1, N2 and N3 [19,23,25], the compound N4 was more active on all forms of *T. cruzi* and seems to have earlier harmful effects on mitochondria. This perspective suggests that shorter treatment times can be an alternative to increase the selectivity of the compound and to avoid the high toxicity observed for the others naphthoimidazoles [21].

Our data pointed that complexes II-III were primarily affected by ROS during the treatment, while the damage caused in complex IV occurs as a secondary step and after longer treatment. Succinate dehydrogenase uses the oxidized form of ubiquinone as an electron acceptor [57], and the steric hindrance in this binding site may prevent the oxidation-reduction cycle of quinoid ring. This process can increase the unstable semiquinone pool [58] and may explain the high ROS amounts detected early. These experimental data were reinforced by theoretical analysis, as the molecular docking results suggested that the ubiquinone site in succinate dehydrogenase is the main binding pocket for N4 due to the long alkyl chain of the naphtoimidazolium under study.

On the other hand, the favorable docking score value between N4 and DHODH opens new perspectives into the mechanism of action of this naphthomidazole. This enzyme participates in *de novo* biosynthesis of pyrimidine and has been described as a promising chemotherapeutic target, as it markedly differs from the human enzyme [59,60]. It was previously demonstrated that the disruption of DHODH and *de novo* pyrimidine biosynthesis pathway led to the gradual death of *T. cruzi* [61,62]. Coupled with orotate oxidation, DHODH also reduces fumarate to succinate. Once our results pointed to early mitochondrial damage, we cannot discard the role as a soluble fumarate reductase occupied by DHODH [59] and the consequences of a steric hindrance caused by N4 in succinate pool. This molecule is largely produced as an end product of glucose degradation and enters the ETS through a NADH-dependent fumarate reductase [41,63]; however, little is known about the contribution of succinate produced by DHODH to ETS and mitochondrial physiology. Additionally, the ultrastructural observation of parasites with mitotic phenotype, such as two flagella, nuclei or kinetoplasts, was frequently detected after the treatment with N4, indicating interference in the parasite cell cycle, as previously reported in epimastigotes treated with the three naphthoimidazoles (N1, N2 and N3) and with triazolic derivatives of the naphthoquinone [23,64]. However, due to the direct effect of N4 on DHODH, the indirect effect on DNA duplication derived from the decrease in pyrimidine amounts must be further investigated in future.

In conclusion, the strong trypanocidal effect of N4 is dependent on mitochondrial ROS production, involving damage to complexes II-III in the first hours and extensive injury to the mitochondria (morphological and functional) after 24 h, unlike what was observed for the other naphthoimidazoles. According to computational docking, because van der Waals forces are the main interactions between N4 and the enzymes, the insertion of aliphatic chains in the structure of naphthoimidazole **3** has been shown to have an essential role in trypanocidal activity improvement. The compiled data presented here showed the high efficacy of N4 and highlighted the importance of new treatment models for the subsequent evaluation of selectivity, toxicity and tolerance in mammals.

## Funding

This work was supported by CNPq (Universal and PAPES VI), CAPES, FAPERJ (APQ1), PDTIS/FIOCRUZ and FIOCRUZ.

## Declaration of Competing Interest

The authors declare that they have no known competing financial interests or personal relationships that could have appeared to influence the work reported in this paper.

## Acknowledgements

We are very thankful to Marcos Meuser and Robertson Girão for their excellent technical support and to Drs. Solange L. de Castro and Eufranio Silva Junior for the helpful discussions.

## Appendix A. Supplementary data

Supplementary material related to this article can be found, in the online version, at doi:https://doi.org/10.1016/j.biopha.2020.111186.

## References

[1] J.C.P. Dias, A.N. Ramos, E.D. Gontijo, A. Luquetti, M.A. Shikanai-Yasuda, J. R. Coura, R.M. Torres, J.R.D.C. Melo, E.A. De Almeida, W. De Oliveira Junior, A. C. Silveira, J.M. De Rezende, F.S. Pinto, A.W. Ferreira, A. Rassi, A.A. Fragata Filho, A.S. De Sousa, D. Correia, A.M. Jansen, G.M.Q. Andrade, C.F. De Paoli de Carvalho Britto, A.Y.D.N. Pinto, A. Rassi Junior, D.E. Campos, F. Abad-Franch, S.E. Santos, E. Chiari, A.M. Hasslocher-Moreno, E.F. Moreira, D.S.D.O. Marques, E.L. Silva, J. A. Marin-Neto, L.M.D.C. Galvão, S.S. Xavier, S.A.D.S. Valente, N.B. Carvalho, A. V. Cardoso, R.A.E. Silva, V.M. Da Costa, S.M. Vivaldini, S.M. Oliveira, V.D. C. Valente, M.M. Lima, R.V. Alves, 2nd Brazilian consensus on chagas disease, 2015, Rev. Soc. Bras. Med. Trop. 49 (2016) 3–60, https://doi.org/10.1590/0037-8682-0505-2016.

[2] S. Antinori, L. Galimberti, R. Bianco, R. Grande, M. Galli, M. Corbellino, Chagas disease in Europe: a review for the internist in the globalized world, Eur. J. Intern. Med. 43 (2017) 6–15, https://doi.org/10.1016/j.ejim.2017.05.001.

[3] B. Monge-Maillo, R. López-Vélez, Challenges in the management of Chagas disease in Latin-American migrants in Europe, Clin. Microbiol. Infect. 23 (2017) 290–295, https://doi.org/10.1016/j.cmi.2017.04.013.

[4] D. Silva-dos-Santos, J. Barreto-de-Albuquerque, B. Guerra, O.C. Moreira, L. R. Berbert, M.T. Ramos, B.A.S. Mascarenhas, C. Britto, A. Morrot, D.M. Serra Villa-Verde, L.R. Garzoni, W. Savino, V. Cotta-de-Almeida, J. de Meis, Unraveling Chagas disease transmission through the oral route: gateways to *Trypanosoma cruzi* infection and target tissues, PLoS Negl. Trop. Dis. 11 (2017), https://doi.org/10.1371/journal.pntd.0005507.

[5] L.A. Messenger, C. Bern, Congenital Chagas disease: current diagnostics, limitations and future perspectives, Curr. Opin. Infect. Dis. 31 (2018) 415–421, https://doi.org/10.1097/QCO.0000000000000478.

[6] R.T.B. Ferreira, M.L. Cabral, R.S. Martins, P.F. Araujo, S.A. Da Silva, C. Britto, M. R. Branquinho, P. Cardarelli-Leite, O.C. Moreira, Detection and genotyping of *Trypanosoma cruzi* from açai products commercialized in Rio de Janeiro and Pará, Brazil, Parasit. Vectors 11 (2018), https://doi.org/10.1186/s13071-018-2699-6.

[7] A. Prata, Clinical and epidemiological aspects of Chagas disease, Lancet Infect. Dis. 1 (2001) 92–100, https://doi.org/10.1016/S1473-3099(01)00065-2.

[8] C. Bern, Chagas' disease, N. Engl. J. Med. 373 (2015) 1882.

[9] M.N.C. Soeiro, S.L. De Castro, *Trypanosoma cruzi* targets for new chemotherapeutic approaches, Exp. Opin. Ther. Targets 13 (2009) 105–121, https://doi.org/10.1517/14728220802623881.

[10] J.A. Urbina, Specific chemotherapy of Chagas disease: relevance, current limitations and new approaches, Acta Trop. 115 (2010) 55–68, https://doi.org/10.1016/j.actatropica.2009.10.023.

[11] J.R. Coura, S.L. De Castro, A critical review on chagas disease chemotherapy, Mem. Inst. Oswaldo Cruz 97 (2002) 3–24, https://doi.org/10.1590/S0074-02762002000100001.

[12] E.N. da Silva Júnior, G.A.M. Jardim, C. Jacob, U. Dhawa, L. Ackermann, S.L. de Castro, Synthesis of quinones with highlighted biological applications: a critical update on the strategies towards bioactive compounds with emphasis on lapachones, Eur. J. Med. Chem. 179 (2019) 863–915, https://doi.org/10.1016/j.ejmech.2019.06.056.

[13] P.A. Garavaglia, M.F. Rubio, M. Laverrière, L.M. Tasso, L.E. Fichera, J.J. B. Cannata, G.A. García, *Trypanosoma cruzi*: Death phenotypes induced by ortho-naphthoquinone substrates of the aldo-keto reductase (TcAKR). Role of this enzyme in the mechanism of action of β-lapachone, Parasitology 145 (2018) 1251–1259, https://doi.org/10.1017/S0031182018000045.

[14] P. Guiraud, R. Steiman, G.M. Campos-Takaki, F. Seigle-Murandi, M.S. De Buochberg, Comparison of antibacterial and antifungal activities of lapachol and β-lapachone, Planta Med. 60 (1994) 373–374, https://doi.org/10.1055/s-2006-959504.

[15] E.N. da Silva Júnior, G.A.M. Jardim, C. Jacob, U. Dhawa, L. Ackermann, S.L. de Castro, Synthesis of quinones with highlighted biological applications: a critical update on the strategies towards bioactive compounds with emphasis on lapachones, Eur. J. Med. Chem. 179 (2019) 863–915, https://doi.org/10.1016/j.ejmech.2019.06.056.

[16] K.C.G. De Moura, F.S. Emery, C. Neves-Pinto, M.D.C.F.R. Pinto, A.P. Dantas, K. Salomão, S.L. De Castro, A.V. Pinto, Trypanocidal Activity of Isolated Naphthoquinones from Tabebuia and Some Heterocyclic Derivatives: A Review from an Interdisciplinary Study, J. Braz. Chem. Soc. 12 (2001) 325–338, https://doi.org/10.1590/S0103-50532001000300003.

[17] K.C.G. De Moura, K. Salomão, R.F.S. Menna-Barreto, F.S. Emery, M.D.C.F.R. Pinto, A.V. Pinto, S.L. De Castro, Studies on the trypanocidal activity of semi-synthetic pyran[b-4,3] naphtho[1,2-d]imidazoles from β-lapachone, Eur. J. Med. Chem. 39 (2004) 639–645, https://doi.org/10.1016/j.ejmech.2004.02.015.

[18] A.V. Pinto, C.N. Pinto, M.D.C.F.R. Pinto, R.S. Rita, C.A.C. Pezzella, S.L. De Castro, Trypanocidal activity of synthetic heterocyclic derivatives of active quinones from Tabebuia sp, Arzneimittel-Forschung/Drug Res. 47 (1997) 74–79, https://doi.org/10.1002/chin.199723258.

[19] A.C.S. Bombaça, P.G. Viana, A.C.C. Santos, T.L. Silva, A.B.M. Rodrigues, A.C. R. Guimarães, M.O.F. Goulart, E.N. da Silva Júnior, R.F.S. Menna-Barreto, Mitochondrial disfunction and ROS production are essential for anti-*Trypanosoma cruzi* activity of β-lapachone-derived naphthoimidazoles, Free Radic. Biol. Med. 130 (2019) 408–418, https://doi.org/10.1016/j.freeradbiomed.2018.11.012.

[20] G.V.F. Brunoro, V.M. Faça, M.A. Caminha, A.T. da S. Ferreira, M. Trugilho, K.C. G. de Moura, J. Perales, R.H. Valente, R.F.S. Menna-Barreto, Differential gel electrophoresis (DIGE) evaluation of naphthoimidazoles mode of action: a study in *trypanosoma cruzi* bloodstream trypomastigotes, PLoS Negl. Trop. Dis. 10 (2016), https://doi.org/10.1371/journal.pntd.0004951.

[21] C.M. Cascabulho, M. Meuser-Batista, K.C.G. de Moura, M.D.C. Pinto, T.L.A. Duque, K.C. Demarque, A.C.R. Guimarães, P.P. de A. Manso, M. Pelajo-Machado, G. M. Oliveira, S.L. De Castro, R.F.S. Menna-Barreto, Antiparasitic and anti-inflammatory activities of β-lapachone-derived naphthoimidazoles in experimental acute *Trypanosoma cruzi* infection, Mem. Inst. Oswaldo Cruz 115 (2020), https://doi.org/10.1590/0074-02760190389.

[22] R.F.S. Menna-Barreto, K. Salomão, A.P. Dantas, R.M. Santa-Rita, M.J. Soares, H. S. Barbosa, S.L. de Castro, Different cell death pathways induced by drugs in *Trypanosoma cruzi*: an ultrastructural study, Micron 40 (2009) 157–168, https://doi.org/10.1016/j.micron.2008.08.003.

[23] R.F.S. Menna-Barreto, J.R. Correa, A.V. Pinto, M.J. Soares, S.L. de Castro, Mitochondrial disruption and DNA fragmentation in *Trypanosoma cruzi* induced by naphthoimidazoles synthesized from beta-lapachone, Parasitol. Res. 101 (2007) 895–905, https://doi.org/10.1007/s00436-007-0556-1.

[24] R.F.S. Menna-Barreto, D.G. Beghini, A.T.S. Ferreira, A.V. Pinto, S.L. De Castro, J. Perales, A proteomic analysis of the mechanism of action of naphthoimidazoles in *Trypanosoma cruzi* epimastigotes *in vitro*, J. Proteomics 73 (2010) 2306–2315, https://doi.org/10.1016/j.jprot.2010.07.002.

[25] R.F.S. Menna-Barreto, A. Henriques-Pons, A.V. Pinto, J.A. Morgado-Diaz, M. J. Soares, S.L. De Castro, Effect of a beta-lapachone-derived naphthoimidazole on *Trypanosoma cruzi*: identification of target organelles, J. Antimicrob. Chemother. 56 (2005) 1034–1041, https://doi.org/10.1093/jac/dki403.

[26] A.M. Da Silva, L. Araújo-Silva, A.C.S. Bombaça, R.F.S. Menna-Barreto, C. E. Rodrigues-Santos, A.B. Buarque Ferreira, S.L. De Castro, Synthesis and biological evaluation of N-alkyl naphthoimidazoles derived from β-lapachone against *Trypanosoma cruzi* bloodstream trypomastigotes, Med. Chem. Res. 8 (2017) 952–959, https://doi.org/10.1039/c7md00069c.

[27] C.N. Pinto, A.P. Dantas, K.C.G. De Moura, F.S. Emery, P.F. Polequevitch, M.C.F. R. Pinto, S.L. De Castro, A.V. Pinto, Chemical reactivity studies with naphthoquinones from Tabebuia with anti-trypanosomal efficacy, Arzneimittel-Forschung/Drug Res. 50 (2000) 1120–1128, https://doi.org/10.1055/s-0031-1300337.

[28] E.N. da Silva Júnior, M.C.B.V. de Souza, M.C. Fernandes, R.F.S. Menna-Barreto, M. do C.F.R. Pinto, F. de Assis Lopes, C.A. de Simone, C.K.Z. Andrade, A.V. Pinto, V.F. Ferreira, S.L. de Castro, Synthesis and anti-*Trypanosoma cruzi* activity of derivatives from nor-lapachones and lapachones, Bioorg. Med. Chem. Lett. 16 (2008) 5030–5038, https://doi.org/10.1016/j.bmc.2008.03.032.

[29] T.P. Barbosa, H.D. Neto, Preparação de derivados do lapachol em meio ácido e em meio básico: uma proposta de experimentos para a disciplina de química orgânica experimental, Quim. Nova 36 (2013) 331–334, https://doi.org/10.1590/S0100-40422013000200021.

[30] R.L.S. Gonçalves, R.F.S. Menna Barreto, C.R. Polycarpo, F.R. Gadelha, S.L. Castro, M.F. Oliveira, A comparative assessment of mitochondrial function in epimastigotes and bloodstream trypomastigotes of *Trypanosoma cruzi*, J. Bioenerg. Biomembr. 43 (2011) 651–661, https://doi.org/10.1007/s10863-011-9398-8.

[31] E. Camargo, Growth and Differentiation in *Trypanosoma cruzi*. I. Origin of metacyclic trypanosomes in liquid media, Rev. Inst. Med. Trop. São Paulo 6 (1963) 93–100.

[32] A.C.S. Bombaça, D. Von Dossow, J.M.C. Barbosa, C. Paz, V. Burgos, R.F.S. Menna-Barreto, Trypanocidal activity of natural sesquiterpenoids involves mitochondrial dysfunction, ROS production and autophagic phenotype in trypanosomacruzi, Molecules 23 (2018), https://doi.org/10.3390/molecules23112800.

[33] S.L. de Castro, M.C. Pinto, A.V. Pinto, Screening of natural and synthetic drugs against Trypanosoma cruzi. 1. Establishing a structure/activity relationship, Microbios 78 (1994) 83–90.

[34] M.R. Simões-Silva, A.S.G. Nefertiti, J.S. De Araújo, M.M. Batista, P.B. Da Silva, M. T. Bahia, R.S. Menna-Barreto, B.P. Pavão, J. Green, A.A. Farahat, A. Kumar, D. W. Boykin, M.N.C. Soeiro, Phenotypic screening in vitro of novel aromatic amidines against Trypanosoma cruzi, Antimicrob. Agents Chemother. 60 (2016) 4701–4707, https://doi.org/10.1128/AAC.01788-15.

[35] R.F.S. Menna-Barreto, R.L.S. Goncalves, E.M. Costa, R.S.F. Silva, A.V. Pinto, M. F. Oliveira, S.L. de Castro, The effects on Trypanosoma cruzi of novel synthetic

naphthoquinones are mediated by mitochondrial dysfunction, Free Radic. Biol. Med. 47 (2009) 644–653, https://doi.org/10.1016/j.freeradbiomed.2009.06.004.
[36] C.J. Hamilton, A. Saravanamuthu, I.M. Eggleston, A.H. Fairlamb, Ellman's-reagent-mediated regeneration of trypanothione in situ: Substrate-economical microplate and time-dependent inhibition assays for trypanothione reductase, Biochem. J. 369 (2003) 529–537, https://doi.org/10.1042/BJ20021298.
[37] T.V. Votyakova, I.J. Reynolds, Detection of hydrogen peroxide with Amplex Red: interference by NADH and reduced glutathione auto-oxidation, Arch. Biochem. Biophys. 431 (2004) 138–144, https://doi.org/10.1016/j.abb.2004.07.025.
[38] D.K. Inaoka, K. Sakamoto, H. Shimizu, T. Shiba, G. Kurisu, T. Nara, T. Aoki, K. Kita, S. Harada, Structures of Trypanosoma cruzi dihydroorotate dehydrogenase complexed with substrates and products: atomic resolution insights into mechanisms of dihydroorotate oxidation and fumarate reduction, Biochemistry (2008), https://doi.org/10.1021/bi800413r.
[39] V.I. Lushchak, Free radicals, reactive oxygen species, oxidative stress and its classification, Chem. Biol. Interact. 224 (2014) 164–175, https://doi.org/10.1016/j.cbi.2014.10.016.
[40] A.E. Vercesi, C.F. Bernardes, M.E. Hoffmann, F.R. Gadelha, R. Docampo, Digitonin permeabilization does not affect mitochondrial function and allows the determination of the mitochondrial membrane potential of Trypanosoma cruzi in situ, J. Biol. Chem. (1991).
[41] D.A. Maugeri, J.J.B. Cannata, J.J. Cazzulo, Glucose metabolism in Trypanosoma cruzi, Essays Biochem. (2011), https://doi.org/10.1042/BSE0510015.
[42] A.V. Pinto, S.L. De Castro, The trypanocidal activity of naphthoquinones: a review, Molecules 14 (2009) 4570–4590, https://doi.org/10.3390/molecules14114570.
[43] A.V. Pinto, M. do C.F. Pinto, O. Oliveira, Síntese das alfa- e beta-nor-lapachonas, propriedades em meio ácido e reações com N-bromosuccinimida, Acad. Bras. Ciências 54 (1982) 107–114.
[44] K.C.G. Moura, P.F. Carneiro, M.D.C.F.R. Pinto, J.A. Da Silva, V.R.S. Malta, C.A. De Simone, G.G. Dias, G.A.M. Jardim, J. Cantos, T.S. Coelho, P.E.A. Da Silva, E.N. Da Silva, 1,3-Azoles from ortho-naphthoquinones: synthesis of aryl substituted imidazoles and oxazoles and their potent activity against Mycobacterium tuberculosis, Bioorg. Med. Chem. Lett. 20 (2012) 6482–6488, https://doi.org/10.1016/j.bmc.2012.08.041.
[45] I. Cuadrado-Berrocal, G. Guedes, A. Estevez-Braun, S. Hortelano, B. De Las Heras, Biological evaluation of angular disubstituted naphthoimidazoles as anti-inflammatory agents, Bioorganic Med. Chem. Lett. 25 (2015) 4210–4213, https://doi.org/10.1016/j.bmcl.2015.08.002.
[46] R. Abraham, P. Prakash, K. Mahendran, M. Ramanathan, A novel series of N-acyl substituted indole-linked benzimidazoles and naphthoimidazoles as potential anti inflammatory, anti biofilm and anti microbial agents, Microb. Pathog. 114 (2018) 409–413, https://doi.org/10.1016/j.micpath.2017.12.021.
[47] L.P. Corrêa Barros, K.P. Del Rio, Tdos S.C. Carvalho, Mdo C.F.R. Pinto, K.C.G. de Moura, P.C.B. Halicki, D.F. Ramos, P.E.A. da Silva, Anti-Mycobacterium tuberculosis activity of naphthoimidazoles combined with isoniazid and rifampicin, Tuberculosis (2018), https://doi.org/10.1016/j.tube.2018.06.015.
[48] C. McKeever, M. Kaiser, I. Rozas, Aminoalkyl derivatives of guanidine diaromatic minor groove binders with antiprotozoal activity, J. Med. Chem. (2013), https://doi.org/10.1021/jm301614w.
[49] M.A. Ismail, R.K. Arafa, R. Brun, T. Wenzler, Y. Miao, W.D. Wilson, C. Generaux, A. Bridges, J.E. Hall, D.W. Boykin, Synthesis, DNA affinity, and antiprotozoal activity of linear dications: Terphenyl diamidines and analogues, J. Med. Chem. (2006), https://doi.org/10.1021/jm060470p.
[50] S. Emami, T. Banipoulad, H. Irannejad, A. Foroumadi, M. Falahati, M. Ashrafi-Khozani, S. Sharifynia, Imidazolylchromanones containing alkyl side chain as lanosterol 14α-demethylase inhibitors: synthesis, antifungal activity and docking study, J. Enzyme Inhib. Med. Chem. (2014), https://doi.org/10.3109/14756366.2013.776554.
[51] R.F.S. Menna-Barreto, S.L. De Castro, The double-edged sword in pathogenic trypanosomatids: the pivotal role of mitochondria in oxidative stress and bioenergetics, Biomed Res. Int. 2014 (2014), https://doi.org/10.1155/2014/614014.
[52] A. Boveris, R. Docampo, J.F. Turrens, A.O. Stoppani, Effect of beta and alpha-lapachone on the production of H202 and on the growth of Trypanosoma cruzi, Rev. Asoc. Argent. Microbiol. 9 (1977) 54–61. http://www.ncbi.nlm.nih.gov/entrez/query.fcgi?cmd=Retrieve&db=PubMed&dopt=Citation&list_uids=339293.
[53] A. Boveris, A.O.M. Stoppani, Hydrogen peroxide generation in Trypanosoma cruzi, Experientia 33 (1977) 1306–1308, https://doi.org/10.1007/BF01920148.
[54] R. Docampo, W. De Souza, F.S. Cruz, I. Roitman, B. Cover, W.E. Gutteridge, Ultrastructural alterations and peroxide formation induced by naphthoquinones in different stages of Trypanosoma cruzi, Zeitschrift Für Parasitenkd, Parasitol. Res. 57 (1978) 189–198, https://doi.org/10.1007/BF00928032.
[55] R.F.S. Menna-Barreto, J.R. Corrêa, C.M. Cascabulho, M.C. Fernandes, A.V. Pinto, M.J. Soares, S.L. De Castro, Naphthoimidazoles promote different death phenotypes in Trypanosoma cruzi, Parasitology 136 (2009) 499–510, https://doi.org/10.1017/S0031182009005745.
[56] B. Halliwell, Reactive species and antioxidants. Redox biology is a fundamental theme of aerobic life, Plant Physiol. (2006), https://doi.org/10.1104/pp.106.077073.
[57] J.W. Peters, D.N. Beratan, B. Bothner, R.B. Dyer, C.S. Harwood, Z.M. Heiden, R. Hille, A.K. Jones, P.W. King, Y. Lu, C.E. Lubner, S.D. Minteer, D.W. Mulder, S. Raugei, G.J. Schut, L.C. Seefeldt, M. Tokmina-Lukaszewska, O.A. Zadvornyy, P. Zhang, M.W. Adams, A new era for electron bifurcation, Curr. Opin. Chem. Biol. (2018), https://doi.org/10.1016/j.cbpa.2018.07.026.
[58] M.P. Murphy, How mitochondria produce reactive oxygen species, Biochem. J. (2009), https://doi.org/10.1042/BJ20081386.
[59] E. Takashima, D.K. Inaoka, A. Osanai, T. Nara, M. Odaka, T. Aoki, K. Inaka, S. Harada, K. Kita, Characterization of the dihydroorotate dehydrogenase as a soluble fumarate reductase in Trypanosoma cruzi, Mol. Biochem. Parasitol. (2002), https://doi.org/10.1016/S0166-6851(02)00100-7.
[60] M. Pinto Pinheiro, F. da Silva Emery, M. Cristina Nonato, Target sites for the design of anti-trypanosomatid drugs based on the structure of dihydroorotate dehydrogenase, Curr. Pharm. Des. (2013), https://doi.org/10.2174/1381612811319140011.
[61] T. Annoura, T. Nara, T. Makiuchi, T. Hashimoto, T. Aoki, The origin of dihydroorotate dehydrogenase genes of kinetoplastids, with special reference to their biological significance and adaptation to anaerobic, parasitic conditions, J. Mol. Evol. (2005), https://doi.org/10.1007/s00239-004-0078-8.
[62] M. Hashimoto, J. Morales, Y. Fukai, S. Suzuki, S. Takamiya, A. Tsubouchi, S. Inoue, M. Inoue, K. Kita, S. Harada, A. Tanaka, T. Aoki, T. Nara, Critical importance of the de novo pyrimidine biosynthesis pathway for Trypanosoma cruzi growth in the mammalian host cell cytoplasm, Biochem. Biophys. Res. Commun. (2012), https://doi.org/10.1016/j.bbrc.2011.12.073.
[63] A. Boveris, C.M. Hertig, J.F. Turrens, Fumarate reductase and other mitochondrial activities in Trypanosoma cruzi, Mol. Biochem. Parasitol. (1986), https://doi.org/10.1016/0166-6851(86)90121-0.
[64] M.C. Fernandes, E.N. Da Silva, A.V. Pinto, S.L. De Castro, R.F.S. Menna-Barreto, A novel triazolic naphthofuranquinone induces autophagy in reservosomes and impairment of mitosis in Trypanosoma cruzi, Parasitology 139 (2012) 26–36, https://doi.org/10.1017/S0031182011001612.